On the calibration of a WEC-Sim model for heaving point absorbers

Tosdevin, T

On the calibration of a WEC-Sim model for heaving point absorbers.

Tom Tosdevin*[1], Marianna Giassi[2], Simon Thomas[2],
Jens Engström[2], Martyn Hann[1], Jan Isberg[2], Malin Göteman[2], Edward Ransley[1], Pierre-Henri Musiedlak[1],
Dave Simmonds[1], Deborah Greaves[1]

[1] School of Science and Engineering, University of Plymouth,
Plymouth, Devon PL4 8AA, UK
*E-mail: Tom.Tosdevin@postgrad.plymouth.ac.uk
[2] Department of Engineering Science, Uppsala University
Box 534, 751 21 Uppsala, Sweden

Abstract— **The outcomes of reliability based design methods applied to wave energy converters (WECs) in the early stages of development depend heavily on the uncertainty in the variables used to determine the loads acting on, and responses of, devices. Open source software has been developed in recent years to aid in the response modelling of devices such as NEMOH, WEC-Sim and OpenFOAM. Uncertainty in the estimation of the viscous drag forces acting on a device has been identified as a key source of error in diffraction and radiation based hydrodynamic models. Different methods of determining the drag coefficient are compared in the case of 2 heaving point absorbers in the absence of PTOs.**

This study uses physical model decay tests to try and quantify the viscous damping for the X-MED buoy and Uppsala University's model WEC, a bottom referenced point absorber similar to the full scale Seabased device. The approach is then evaluated by applying the values obtained for the drag coefficients to the hydrodynamic model WEC-Sim which is then compared to physical model tank tests in regular waves.

Keywords—**Wave energy, WEC, Drag, Viscosity, WEC-Sim.**

I. INTRODUCTION

The survivability and reliability of wave energy convertors (WECs) has been identified by industry and researchers as an important area in need of improvement in order to reduce the levelized cost of energy (LCOE) for the technology [1]. The wave energy sector is a marginal industry in which the differences between lifetime costs and revenues of devices is relatively small, a fact which is exacerbated by large capital costs of developments. By looking to other industries in similar situations approaches to improving the reliability and reducing the LCOE for the technology can be identified and adapted. Practices from the offshore oil and gas industry have been adopted by offshore wind farm developers and so the wave and tidal energy development community are well placed to benefit from this work. The RiaSoR (Reliability in a sea of risk) project [1], [2] has identified and adapted probabilistic design methodology from the automotive and aerospace industries to be applied to the development of wave energy technology.

Probabilistic design approaches to improve reliability are based on the quantification of environmental and modelling uncertainties in the load and device responses. Quantifying the uncertainties which relate to the numerical and physical response modelling of devices is therefore an active area of research. This is true of numerical simulations in the form of validation studies [3] and differences in physical testing facilities round robin projects such as those being carried out through MaRINET [4]. Physical tank testing can be costly and time consuming and high fidelity numerical modelling strategies such as computational fluid dynamics (CFD) are impractical for conducting large numbers of repeat simulations that may be useful in the early stages of design.

WEC-Sim [5] is a radiation and diffraction based numerical model that is fast enough for it to be practical to run large numbers of numerical simulations. There are however uncertainties and errors in the model inputs that will affect the outcomes of the simulations. In particular the uncertainty regarding the viscous forces that act on devices have been identified [2] [6] [7] as a key source of uncertainty in potential flow based models. Viscous

dissipation is a well-studied phenomenon which mainly occurs due to viscous friction and vortex shedding [8]. Viscous effects can be included in radiation and diffraction based models in the form of a linear or a quadratic damping term involving a characteristic area and drag coefficient implemented through the Morrison equation. Typically these are determined either from physical [10] [11] [12] or CFD [10] [12] [13] decay tests or by estimates based on device geometry and the Reynolds number [9] [15]. There are clear advantages and disadvantages to each method with the expectation being that physical testing is the most accurate but also the most time consuming and financially costly. This is followed by CFD then estimates from device geometry and the literature. The relative merits of these methods will be explored in order to calibrate a WEC-Sim model. Both devices benefit from a history of previous testing in the University of Plymouth's COAST lab [16].

This work uses experimental data from physical wave tank testing. The focus of the paper is numerical modelling and not to discuss the experiments in detail. For more details on the experimental set-up and results, the reader is referred to [17] [18]. This paper aims to compare the different methods used in determining viscous forces acting on devices and apply them to calibrating a WEC-Sim model using the open source tools NEMOH, WEC-Sim and OpenFOAM. The physical responses of the devices in regular waves are then used to compare the WEC-Sim model to experimental data.

II. Device Descriptions

A. Xmed buoy

The X-MED buoy was designed for the EPSRC project [19] (Extreme loading of marine energy devices due to waves, current, flotsam, and mammal impacts). It was designed to be a generic representation of a heaving point absorber for use specifically in a set of experiments on extreme responses and so is not representative of any one particular full scale WEC in development. The decay tests cited here were carried out as part of this project and other publications using this or a similar configuration can be found in [18] [19] [20]. The set up consisted of a 43.2kg buoy in 2.8m water depth secured to a spring by, 35kN/m stiffness Dyneema rope. The spring is then fixed to the tank bottom by a universal joint so that the buoy can move in 6DoF. This means that the buoy can move in 6DoF during the experimental decay tests but is limited to heave motion only in the CFD and WEC-Sim decay test models. This is not considered to significantly impact the analysis of the viscous terms as the motions observed during the physical decay tests in all DOF other than heave were slight.

The X-MED buoy geometry consists of a 0.5m diameter 0.25m high cylinder atop a 0.25m radius hemisphere (See Fig. 1) this is a simple geometry and so a mesh of the device can be created with high confidence in its accuracy.

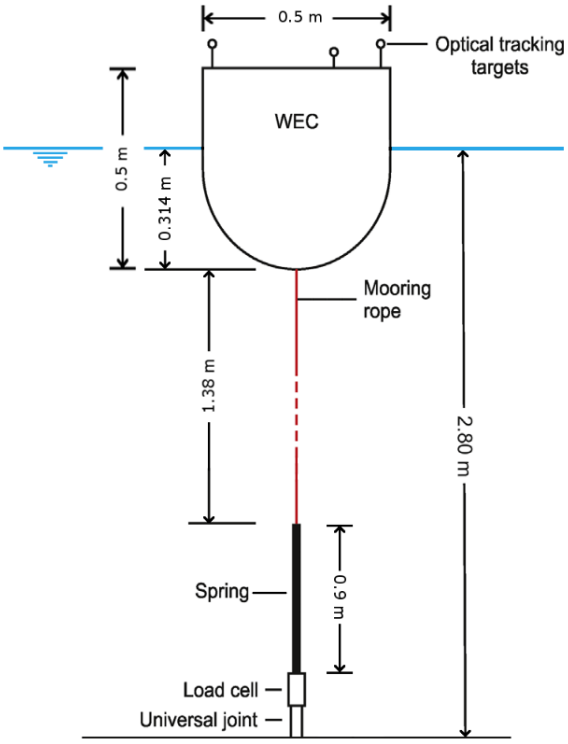

Fig. 1. X-MED buoy experimental setup for the heave decay test. Taken from [18]

B. Uppsala buoy

The other WEC to be used in this analysis was developed by Uppsala University. It is a point absorber that generates due to heave and surge motions, it consists of a buoy attached via a line to a linear generator on the sea bed secured by a gravity base foundation (See Fig. 2).

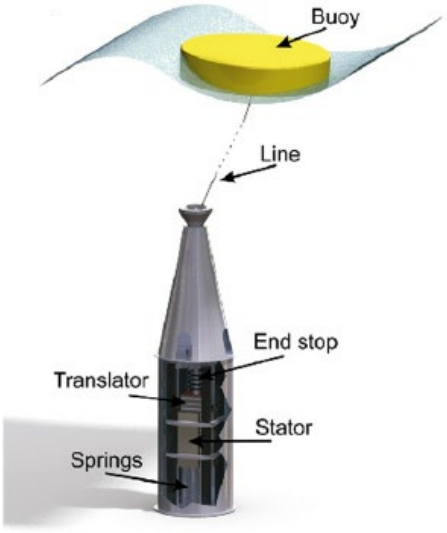

Fig. 2. Uppsala full scale device. Taken from [21]

The WEC tests were performed on a 1:10 scale model of the buoy with a diameter of 0.488m, height of 0.28m, and

mass of 4.378kg. A pulley system connected a suspended 5kg mass, situated outside of the basin, to the buoy to provide a pre-tension. Decay tests were also performed for the buoy with no mass attached and with 10kg. The details of the experimental set-up are similar to those found in [17] but with the PTO absent. The physical tests analysed here were conducted without any PTOs, this has the advantage of simplifying the models and removing the uncertainties involved in modelling the PTOs but the disadvantage that the results are not representative of the devices in operational mode. Therefore, no conclusions about power output can be made. This also has implications for determining the drag coefficient in operational mode as [22] note that PTO control strategies increase the relative velocity and so can greatly alter the viscous effects.

In this analysis the Uppsala buoy has been modelled as two 9.5cm high spherical caps separated by a 9cm high, 0.488cm diameter cylinder as shown in Fig 4.

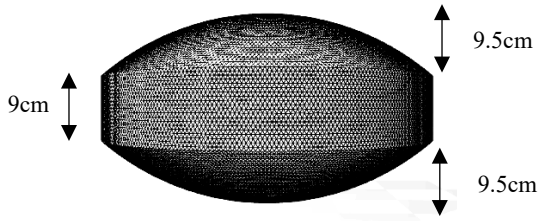

Fig. 3. Uppsala buoy mesh.

III. NUMERICAL MODELLING TOOLS.

In order to use frequency domain boundary element method (BEM) solvers such as NEMOH to numerically model the motions of WECs in the time domain, the Cummins equation is used which can be defined and solved numerically with a set of ordinary differential equations [23]. NEMOH calculates the hydrodynamic coefficients: the added mass, radiation damping and hydrostatic stiffness. These inputs are required by time domain solvers such as WEC-Sim to calculate the responses of the buoy to the waves via the Cummins equation, given by:

$$m\ddot{X} = F_{exc}(t) + F_{rad}(t) + F_{PTO}(t) + F_v(t) + F_{ME}(t) + F_B(t) + F_m(t) \quad (1)$$

Where $\ddot{X}$ is the acceleration vector of the buoy, m is the mass matrix, F_{exc} is the wave excitation force, $F_{rad}(t)$ is the force vector as a result of the radiated wave, $F_{PTO}(t)$ is the force due to the power take off (PTO), $F_v(t)$ is the damping force vector, $F_{ME}(t)$ is the Morrison Element force vector, $F_B(t)$ is the buoyancy force, and $F_m(t)$ is the force vector due to the moorings. $F_{exc}(t)$, $F_{rad}(t)$ and $F_B(t)$ are calculated from the hydrodynamic coefficients calculated by NEMOH. $F_{rad}(t)$ is dependent on the added mass and damping matrices $A(\omega)$ and $B(\omega)$ [5].

WEC-Sim has the capability to incorporate weak nonlinearities in the form of Froude-Krylov and hydrostatic stiffness terms which relate to the wave excitation and buoyancy [24]. These are implemented by WEC-Sim with the aid of an STL mesh. In the case of the X-MED buoy the cross-sectional area of the wetted surface does not change significantly and so the inclusion of these nonlinearities makes only minor differences to the numerical model outputs. The Uppsala buoy however has a flatter base and so these nonlinearities appear to be more important as the hydrostatic stiffness term changes with the changing wetted cross-sectional area.

The CFD model data used in this analysis were conducted by [18] using OpenFOAM (version 4.1) to solve the two phase, incompressible, Reynolds-Averaged Navier-Stokes (RANS) equations. The flow was considered laminar.

IV. METHODOLOGY

1) Determining viscous effects - linear

Viscous effects can be represented linearly by way of a damping term. This can be determined from experimental decay tests and NEMOH by applying the log-decrement method to determine the total damping of the experimental motions and subtracting from it the radiation damping calculated in NEMOH. The resulting damping term is an estimate of the viscous damping on the buoy (in the absence of friction in the line and drag in the moorings) [25].

2) Determining viscous effects - Non-linear

The non-linear viscous damping is implemented in WEC-Sim by way of the Morrison equation [26].

$$F_v = -C_v\dot{X} - \frac{C_d\rho A_d}{2}\dot{X}\left|\dot{X}\right| \quad (2)$$

Where C_v is the linear damping term, $\dot{X}$ is the buoy velocity, C_d is the drag coefficient and A_d is the characteristic area. The characteristic area is taken as the buoy cross-sectional area in a particular degree of freedom. The drag co-efficient is dependent on the type of flow around the device and is commonly characterised by the Reynolds number and the geometry; it is most accurately determined experimentally.

Estimates of the drag coefficients can sometimes be obtained for simple geometries by determination of the Reynolds (Re) and Keulegan-Carpenter (KC) numbers and comparison to previous experiments.

$$Re = 2\pi \frac{A}{T} \rho L \tag{3}$$

$$KC = 2\pi \frac{A}{D} \tag{4}$$

$$\beta = \frac{Re}{KC} \tag{5}$$

Where A is the motion amplitude, T is the period, L is the characteristic length of the device and D is the diameter. The Sarpkaya Beta term, β, is often included in plots to provide extra information on the evolution of the flow [27]. These dimensionless terms give an indication of the type of flow around a body. However, while this approach has been used often in offshore structural engineering, in the determination of the drag on cylinders in constant flow for example [27], such an approach requires vast amounts of experimental data that has not been gathered in the case of WECs.

Alternatively the linear BEM solver outputs (NEMOH in this instance) can be used in conjunction with several estimated drag coefficients. In this case a least squares curve fitting method implemented to determine which best fits the experimental or CFD model data [11].

Drag coefficients can also be tuned from response amplitude operators (RAOs) calculated from experimental data in regular waves. An approach followed in [28].

$$RAO = \frac{Amplitude\ of\ buoy\ in\ heave}{Amplitude\ of\ the\ encountered\ wave} \tag{6}$$

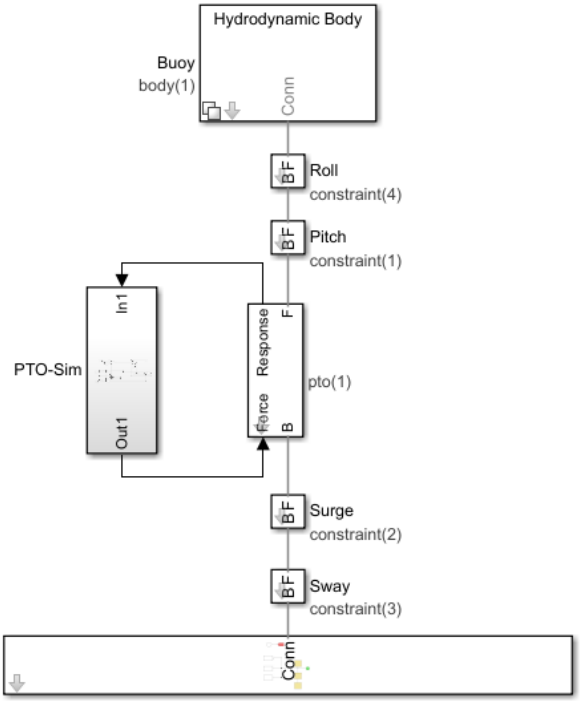

Fig. 4. WEC-Sim Simulink model configuration.

The WEC-Sim model was similar for both devices using constraints to allow movement in 5 degrees of freedom (DOF), surge, sway, heave, roll and pitch. Although there is only very limited motions in roll and sway in the experimental data and so they can be safely ignored. The constraints were removed for the numerical decay tests so that the devices could only move in heave. The X-MED buoy has a spring modelled with a PTO block and a stiffness term of 66.3N/m, the pre-tension enacted by the initial extension of the spring is modelled at the PTO using a pre-tension of 17.9N for the decay tests and 23.4N for the regular wave runs. This difference is due to the decay and regular wave tests being conducted on two separate occasions with slightly different initial spring extensions. The model for the Uppsala WEC is slightly more complicated in that the inertia of the 5kg mass at the end of the tether also had to be included. This is achieved by applying a constant force due to the weight of the 5kg mass at the PTO and a force proportional to the acceleration due to the inertia of the 5kg mass. This is done by editing the PTO actuation force block in Simulink. In both cases the line was modelled as inelastic.

V. RESULTS AND DISCUSSION

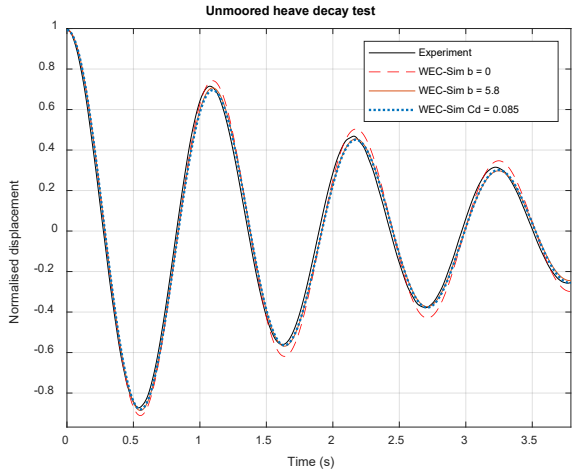

Fig. 5. X-MED unmoored normalised heave decay test. Initial displacement of 18.4cm.

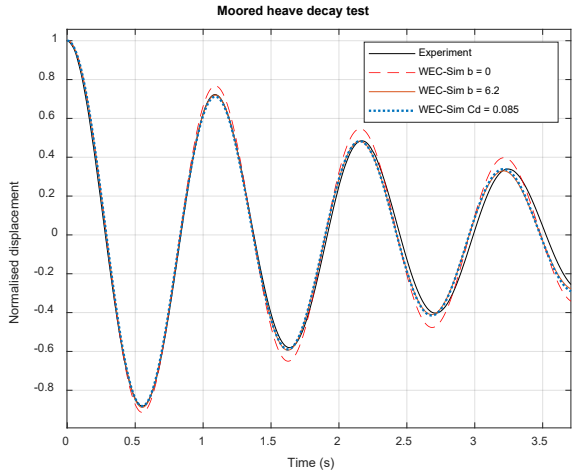

Fig. 6. X-MED moored normalised heave decay test. Initial displacement of 20.37cm.

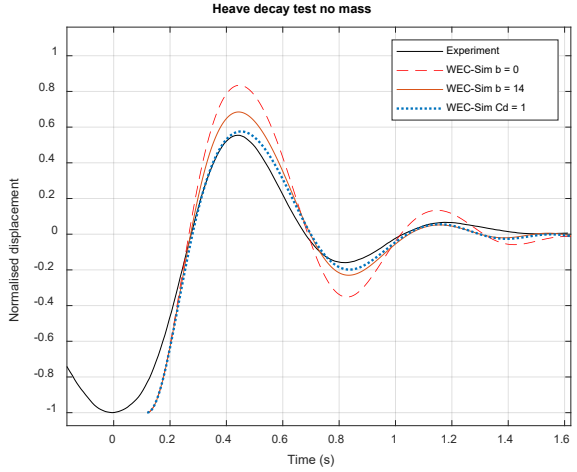

Fig. 7. Uppsala normalised heave decay test, no mass attached. Initial displacement of 4.59cm.

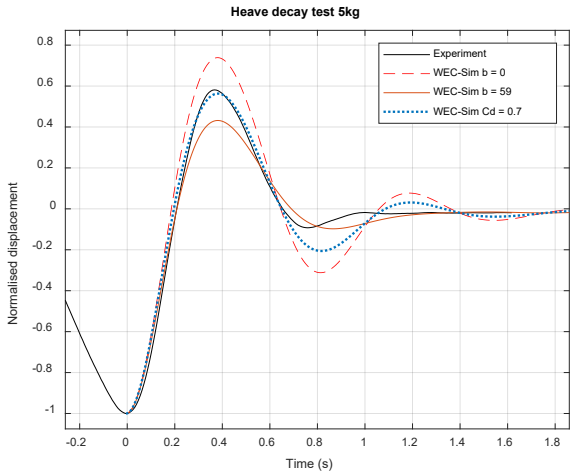

Fig. 8. Uppsala normalised heave decay test, 5kg mass attached. Initial displacement of 8.22cm.

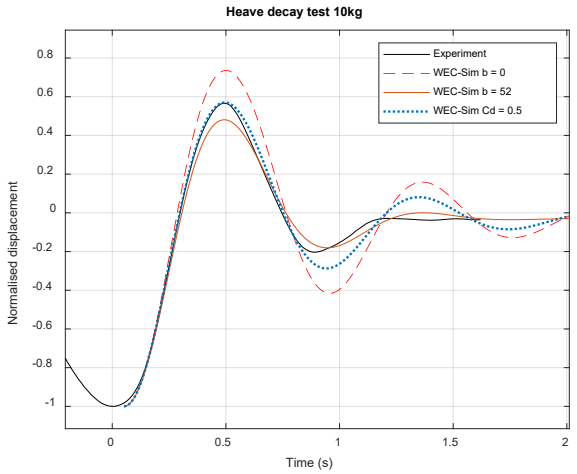

Fig. 9. Uppsala normalised heave decay test, 10kg mass attached. Initial displacement of 13.57cm.

For the nonlinear analysis of the X-MED buoy trial and error was first used to determine a value for the drag coefficient which roughly replicated the experimental results. The coefficient was then varied by steps of 0.005 and a least squares method used to determine the curve that best fit the data over the first 5 cycles. This process was repeated for the CFD decay test and the linear and quadratic coefficients were obtained. It can be seen from table 1 and figures 5 and 6 that the difference between the linear and nonlinear drag terms is minor and that the analysis of the CFD data yields the same drag coefficients and similar linear damping values. The linear and quadratic damping terms are implemented separately in this work i.e. when the linear term is non-zero the quadratic term is zero and vice-versa.

TABLE 1
X-MED HEAVE DECAY

X-MED	Linear damping b (Ns/m)	Drag coefficient C_d
Moored experiment $A_0 = 20.37cm$	6.2	0.085
Moored CFD $A_0 = 20.37cm$	4.4	0.085
Unmoored experiment $A_0 = 18.4cm$	5.8	0.085
Unmoored CFD $A_0 = 18.4cm$	5.2	0.085

In the case of the Uppsala buoy the curves have been plotted so that the phase matches the amplitude of the first peak. For this reason it is not appropriate to perform any curve fitting as the initial position is somewhat arbitrary. The numerical model for the decay test with no mass attached does not fit the experimental data very well initially compared with the 5kg and 10kg cases (see Fig 7, 8, 9). This is thought to be due to the water being in motion at the beginning of the decay tests (the line connecting the mass to the buoy was pulled down and immediately released to perform the test) which has a greater effect in the case when the mass of the system is lower. It is for this reason; the numerical model starting from still water, that the starting point was chosen so that the phase matched the first peak. The accuracy of the log-decrement method reduces for systems that are highly damped [25] and only one cycle could be used for the analysis in the case of the Uppsala buoy. For this reason a large error should be assumed. The linear method is included in the analysis in Fig. 7 – 9 however to illustrate how the linearly damped case compares to the non-linear case.

TABLE 2
UPPSALA HEAVE DECAY

Uppsala	Linear damping b (Ns/m)	Drag coefficient C_d
0kg experiment, $A_0 = 4.59cm$	14	1
5kg experiment $A_0 = 8.22cm$	59	0.7
10kg experiment $A_0 = 13.57cm$	52	0.5

Initial CFD simulations did not appear to fit the experimental data much better than the un-calibrated WEC-Sim model and so have not been included for the Uppsala buoy analysis. The reasons for this will be discussed in the next section.

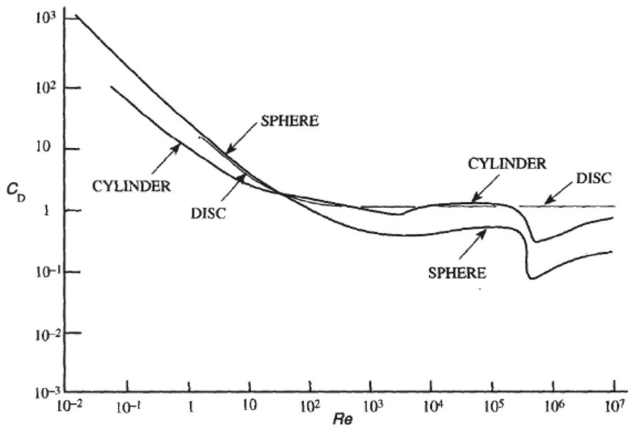

Fig. 10. Drag coefficient versus Reynolds number. Modified from [29].

Fig. 10 illustrates how the drag coefficient changes with Re number for a submerged cylinder, sphere or disk in a constant flow. This evolution of the drag term with Re is explained in terms of the development of the flow around an object as illustrated in Fig. 11. It has been noted [22] that the majority of the literature is concerned with steady flow around fully submerged cylinders and therefore the exact location of the transition or 'critical' region must be taken as a rough guide only when considering oscillatory flow around a semi-submerged buoy.

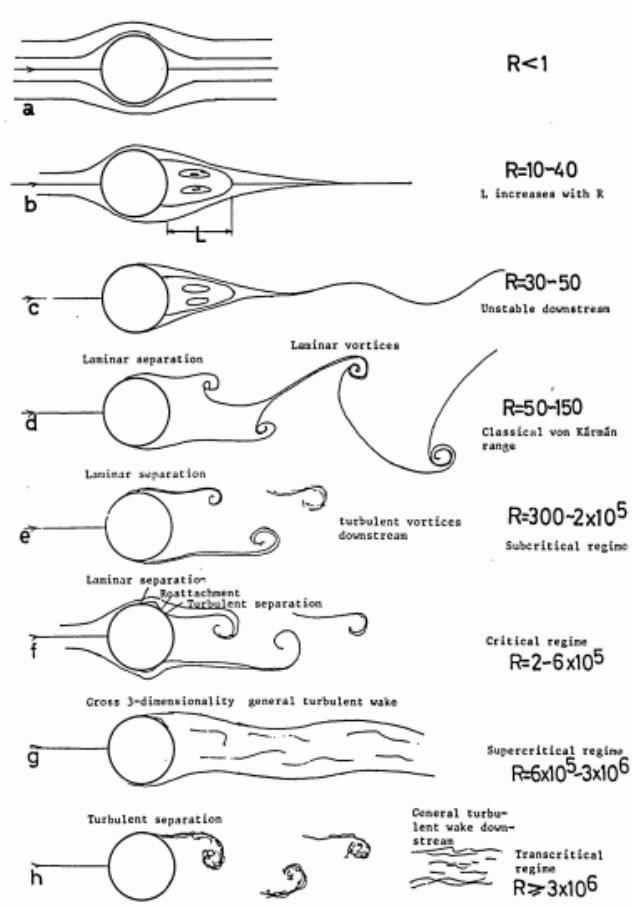

Fig. 11. Flow development with Reynolds number for submerged cylinders in steady flow. Taken from [30].

TABLE 3
UPPSALA REYNOLDS AND KC VALUES DURING CYCLE 1.
$\beta = 3.18 \times 10^5$

Uppsala	Re	KC
No mass A1	1.04×10^5	0.33
5kg A1	1.95×10^5	0.62
10kg A1	3.14×10^5	0.99

TABLE 4
X-MED REYNOLDS AND KC VALUES DURING CYCLES 1 -3.
$\beta = 2.33 \times 10^5$

X-MED	Re	KC
Moored A1	5.23×10^5	2.25
Moored A2	3.45×10^5	1.48
Moored A3	2.4×10^5	1.03
Unmoored A1	4.69×10^5	2.02
Unmoored A2	3.01×10^5	1.29
Unmoored A3	2.03×10^5	0.87

It can be seen that the Re numbers for both the Uppsala and X-MED buoy decay tests potentially lie in the critical region where flow transitions from laminar to turbulent. The exact location of the transition region will be different for the devices as they have different geometries. This fact presents an alternative explanation as to why the CFD and WEC-Sim nonlinear drag models fail to replicate the experimental data as accurately for the Uppsala buoy. A comparison of laminar and turbulent CFD codes applied to heave decay tests in [14] appears to support this explanation as it also found that the laminar model over predicted the motion amplitudes. The CFD model used in this study does not implement any turbulence model and the transition region is particularly difficult to model accurately [31]. There are many different turbulence models, as discussed, for example, in [32] [33]. These have differing strengths and weaknesses, and more thorough analysis and experimental validation is required to determine the most appropriate model for different systems and settings. Such experimental data, including decay or multiple regular wave tests for one particular mass setup with a range of initial displacements and Re numbers, is however not available at this stage. CFD modelling with a RANS k-epsilon turbulence model was carried out for the Uppsala buoy in [34]. However, a different experimental setting than the one discussed here was considered, which obstructs a direct comparison.

In the case of the X-MED buoy the quadratic viscous drag coefficient is very low. However there are cases reported in the literature for similar geometries where the viscous effects can be minimal [14] [35]. [35] Notes that the ratio of the diameter to the draft gives a good indication as to the importance of the viscous effects with a large $2r/d$ being associated with a large drag term. Where d is the draft and r the radius of the buoy. They note that viscous effects can be neglected for some geometries with low $2r/d$ ratios.

RAOs

Another method for selecting a drag coefficient is to compare the numerical model RAOs to experimentally obtained values and tune the Cd values to the data [28]. The experimental run analysed for the Uppsala buoy is for a regular wave with a height of 0.124m and period of 1.11 seconds.

TABLE 5
UPPSALA HEAVE AND SURGE RAO WITH CHANGING CD

Surge Cd	Heave Cd	Heave RAO	Surge RAO	Surge offset (cm)
0	0	0.83	1.4	-0.05
0.7	0.7	0.66	1.32	5.7
1	0.7	0.65	1.3	7.4
1.3	0.7	0.64	1.29	9

Table 5 shows the effect of changing the surge drag coefficient while holding the value in heave, estimated based on the decay test, constant at 0.7. The RAOs calculated from the experimental data are a heave RAO of 0.74 and 1.08 in surge. The buoy oscillates in surge between 0 (its rest position) and 14cm. More data is available for the X-MED buoy and Fig. 12 shows the heave and surge RAOs obtained. Altering the Cd in surge in this case does little to reduce the Surge RAO but has a big impact on the surge offset, the minimum surge position the buoy returns to in regular waves. The experimental value of this offset is close to zero and for this reason it does not make sense to increase the value of Cd in surge until the RAO is tuned to that found in the experiment. This offset is also heavily altered by the inclusion or exclusion of the nonlinearities in the form of the Froude-Krylov and changing hydrostatic stiffness terms.

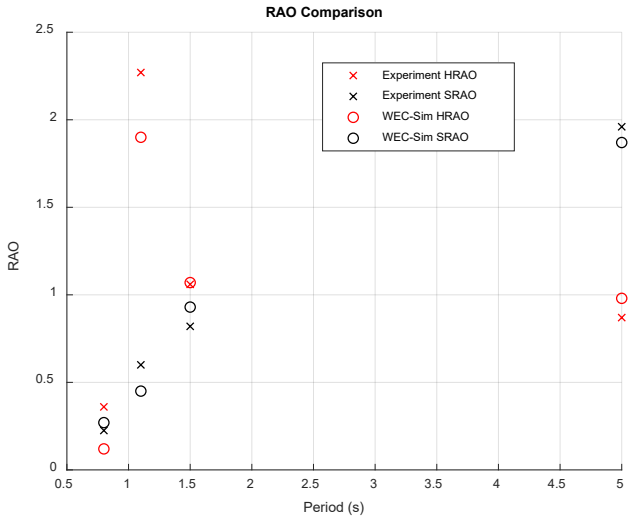

Fig. 12. Heave and surge RAOs for the X-Med buoy in regular waves.

It can be seen from Fig. 12 that the calibrated WEC-Sim model for the X-MED buoy fits the experimental data reasonably well. A surge drag coefficient of 1 was tuned using the experimental data, it can be seen that sometimes this value over predicts the motions and sometimes under predicts them. The pitch motions are not damped in this analysis. It should be noted that because the motions are coupled, differences in the surge, heave or pitch motions have an effect on other DOF.

The larger discrepancy in the heave motions for regular waves with periods T = 0.8s and T = 1.1s appear be due to discrepancies in the surge offset as presented in Fig. 13. This behaviour is not present for the periods T = 1.5s and T = 5s.

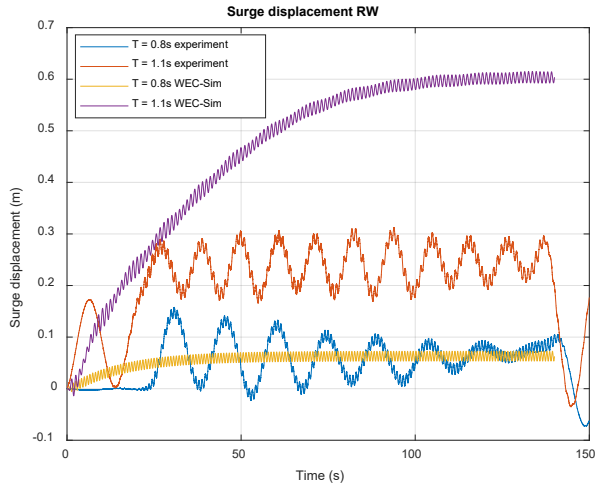

Fig. 13. Surge displacement comparison between experimental and WEC-Sim data for the X-MED buoy.

The higher mode surge oscillations appear to be impacting the heave magnitudes. Without high confidence in the surge drag coefficients it is hard to comment on whether this behaviour not appearing in the WEC-Sim results is due to nonlinearities not included in the model or from errors in the Cd. The heave natural period is calculated to be at T = 1.07s. Either way, resonance and higher order effects can complicate the tuning of the drag coefficients using regular waves.

VI. Conclusions and Future Development

In the case of the X-MED buoy the viscous effects are small and could reasonably be estimated from a CFD model without a turbulence model and implemented in WEC-Sim linearly. There was not a huge difference between the linear and non-linear approach to applying the viscous forces. The CFD simulation provides a useful alternative to the experimental decay tests in the case of low viscous effects. CFD modelling in cases where viscous effects play a larger role and a turbulence model is required is more complex. Therefore cases where viscosity is important are more heavily dependent on expert knowledge and experience to produce accurate results from which to estimate the drag coefficient.

The Uppsala buoy set up was slightly more complicated to model and it is clear from the discrepancies between the physical and numerical results that the model presented here is in need of improvement. Whereas the heave RAO was reasonably accurate for the Uppsala device the surge RAO and offset were significantly different (See Table5) and the offset in particular was inaccurate. It is also unclear to what extent the differences in the drag term between the 0kg, 5kg and 10kg mass decay cases is down to changes in viscous effects due to the changing geometry, initial displacement and Re number and how much is due to either physics unaccounted for in the model or unforeseen elements of the physical set-up.

The approach of estimating a drag coefficient from geometry, previous experiments and the Re number is potentially complicated by the rapid change of Cd with Re in the critical region. More experimental data is required to explore this further and surge decay tests in particular would provide useful additional data.

References

[1] P. Johannesson. “Reliability Guidance for Marine Energy Converters,” RiaSoR (Reliability in a sea of risk). December 2016. [Online] Available: http://riasor.com/wp-content/uploads/2016/12/ReliabilityGuidanceMECs_v1.0_20161216.pdf

[2] M. Atcheson. “Outline load assessment numerical tool,” RiaSor2 (Reliability in a sea of risk)., May 2018. [Online] Available: http://riasor.com/wp-content/uploads/2018/07/201805-RiaSoR-2-Outline-Load-Assessment-Numerical-Tool-Specification.pdf

[3] F. F. Wendt, Y. H. Yu, K. Nielsen, K. Ruehl, T. Bunnik, I. Touzon, B. W. Nam, J. S. Kim, C. E. Janson, K. R. Jakobsen, and S. Crowley, “International energy agency ocean energy systems task 10 wave energy converter modeling verification and validation” National Renewable Energy Lab.(NREL), Golden, CO (United States). (No. NREL/CP-5000-68465). 2017.

[4] D. Noble, S. Draycott, S.Ordonez, K. Porter, C. Johnstone, S.Finch, F. Judge, C. Desmond, B. Santos Varela, J. Lopez Mendia, D. Darbinyan, F. Khalid, L. Johanning, M. Le Boulluec, A. Schaap, “Test recommendations and gap analysis report” MaRINET2 [Online] Available: https://www.researchgate.net/profile/Sam_Draycott/publication/325781217_Test_recommendations_and_gap_analysis_report_MaRINET2_Deliverable_21/links/5b239304a6fdcc697465593a/Test-recommendations-and-gap-analysis-report-MaRINET2-Deliverable-21.pdf?origin=publication_detail

[5] "WEC-Sim (Wave Energy Converter SIMulator) — WEC-Sim documentation", *Wec-sim.github.io*, 2019. [Online]. Available: https://wec-sim.github.io/WEC-Sim/. [Accessed: 25- Feb- 2019].

[6] A. Babarit, J. Hals, M. Muliawan, A. Kurniawan, T. Moan and J. Krokstad, "Numerical benchmarking study of a selection of wave energy converters", *Renewable Energy*, vol. 41, pp. 44-63, 2012.

[7] Y. H. Yu, and Y. Li, "Reynolds-Averaged Navier–Stokes simulation of the heave performance of a two-body floating-point absorber wave energy system," Computers & Fluids, vol. 73, pp.104-114, 2013.

[8] M. A. Bhinder, A. Babarit, L. Gentaz, and P. Ferrant, "Assessment of viscous damping via 3d-cfd modelling of a floating wave energy device," in Proceedings of the 9th European Wave and Tidal Energy Conference, Southampton, UK, 2011.

[9] J. van Rij, Y. H. Yu, K. Edwards and M. Mekhiche, "Ocean power technology design optimization," *International Journal of Marine Energy*, vol. 20, pp.97-108, 2017.

[10] J. Mahesh, N. Seeninaidu, S. Bhattacharya, "CFD simulation and experimental studies on frequency and amplitude dependency of heave damping of spar hull with and without heave plate" International conference on computational and experimental marine hydrodynamics, Chennai, India, December 2014.

[11] B. Guo, R. Patton, S. Jin, J. Gilbert and D. Parsons, "Nonlinear Modeling and Verification of a Heaving Point Absorber for Wave Energy Conversion", IEEE Transactions on Sustainable Energy, vol. 9, no. 1, pp. 453-461, 2018.

[12] S. Jin, R. Patton and B. Guo, "Viscosity effect on a point absorber wave energy converter hydrodynamics validated by simulation and experiment", *Renewable Energy*, vol. 129, pp. 500-512, 2018. Available: 10.1016/j.renene.2018.06.006.

[13] B. Devolder, V. Stratigaki, P. Troch and P. Rauwoens, "CFD Simulations of Floating Point Absorber Wave Energy Converter Arrays Subjected to Regular Waves", *Energies*, vol. 11, no. 3, p. 641, 2018.

[14] H. Gu, P. Stansby, T. Stallard and E. Carpintero Moreno, "Drag, added mass and radiation damping of oscillating vertical cylindrical bodies in heave and surge in still water", *Journal of Fluids and Structures*, vol. 82, pp. 343-356, 2018. Available: 10.1016/j.jfluidstructs.2018.06.012.

[15] J. H. Todalshaug, A. Babarit, A. Kurniawan, and T. Moan, "Numerical estimation of energy delivery from a selection of wave energy converters–final report," The NumWEC project *Ecole Centrale de Nantes & Norges Teknisk-Naturvitenskapelige Universitet*. 2011 [Online] Available: https://www.researchgate.net/publication/275645326_The_NumWEC_project_Numerical_estimation_of_energy_delivery_from_a_selection_of_wave_energy_converters_-_final_report/download

[16] "COAST Plymouth University Marine Engineering Laboratory," 2016

[17] S. Thomas, M. Giassi, M. G¨oteman, M. Hann, E. Ransley, J. Isberg, and J. Engstr¨om, "Performance of a direct-driven wave energy point absorber with high inertia rotatory power take-off," Energies, vol. 11, no. 9, p. 2332, 2018.

[18] P. Musiedlak, E. Ransley, D. Greaves, M. Hann, G. Iglesias, B. Child, "Investigation of model validity for numerical survivability Testing of WECs," in Proceedings of the 12th European Wave and Tidal Energy Conference, Cork, Ireland, 2017.

[19] M. Hann, D. Greaves, and A. Raby, "Snatch loading of a single taut moored floating wave energy converter due to focussed wave groups," Ocean Engineering , vol. 96, pp. 258–271, 2015.

[20] E. Ransley, D. Greaves, A. Raby, D. Simmonds and M. Hann, "Survivability of wave energy converters using CFD", *Renewable Energy*, vol. 109, pp. 235-247, 2017. Available: 10.1016/j.renene.2017.03.003.

[21] J. Engström, M. Eriksson, M. Göteman, J. Isberg and M. Leijon, "Performance of large arrays of point absorbing direct-driven wave energy converters", *Journal of Applied Physics*, vol. 114, no. 20, p. 204502, 2013. Available: 10.1063/1.4833241.

[22] G. Giorgi, and J. V. Ringwood, "Consistency of viscous drag identification tests for wave energy applications," In *Proceedings of the 12th European Wave and Tidal Energy Conference, Cork*. 2017.

[23] W. Cummins, *The impulse response function and ship motions*. [Washington, D.C.]: Dept. of the Navy, David Taylor Model Basin, 1962

[24] M. Lawson, Y.-H. Yu, A. Nelessen, K. Ruehl, and C. Michelen, "Implementing Nonlinear Buoyancy and Excitation Forces in the WEC-Sim Wave Energy Converter Modeling Tool," in Proceedings of the 33rd International Conference on Ocean, Offshore and Arctic Engineering, OMAE 2014, San Francisco, CA, 2014.

[25] S. Chakrabarti, "Basic theory of vibration" in *The theory and practice of hydrodynamics and vibration*. River Edge, N.J.: World Scientific, 2002.

[26] Morison, J.R., M., Johnson, J.W., Schaaf, and S.A., "The force exerted by surface waves on piles," Journal of Petroleum Technology, vol. 2, no. 5, pp. 149–154, May 1950.

[27] J. M. Journée, and W. W. Massie, "Wave forces on slender cylinders" in *Offshore hydromechanics* , TU Delft, 2000.

[28] M. Lawson, B. B. Garzon, F. Wendt, Y. H. Yu, and C. Michelen, 2015, May. "COER hydrodynamic modeling competition: Modeling the dynamic response of a floating body using the WEC-SIM and FAST simulation tools," In *ASME 2015 34th International Conference on Ocean, Offshore and Arctic Engineering*, 2015, pp. V009T09A005-V009T09A005.

[29] R. Caballero, A. Vega, A. Berbey, and M. Armada, "Six degrees of freedom underwater vehicle for culvert inspection," Proceedings of the seventeenth international conference on climbing and walking robots and the support technologies for mobile machines, Poznan, Poland, July 2014.

[30] R.L.P. Verley, "*Oscillations of cylinders in waves and currents"* Ph.D. Thesis, Loughborough University, 1980.

[31] Y. Ono and T. Tamura, "LES of flows around a circular cylinder in the critical Reynolds number region". In *Proceedings of BBAA VI International Colloquium on: Bluff Bodies Aerodynamics and Applications, Milan, Italy*. July 2008.

[32] J. Hart, "Comparison of Turbulence Modeling Approaches to the Simulation of a Dimpled Sphere", *Procedia Engineering*, vol. 147, pp. 68-73, 2016.

[33] M. Tutar, and A. E. Holdø, "Computational modelling of flow around a circular cylinder in sub-critical flow regime with various turbulence models," *International journal for numerical methods in fluids*, *35*(7), pp.763-784. 2001.

[34] L. Sjökvist, J. Wu, E. Ransley, J. Engström, M. Eriksson, and M. Göteman. "Numerical models for the motion and forces of point-absorbing wave energy converters in extreme waves," *Ocean Engineering*, vol. *145*, pp. 1-14, 2017.

[35] Z. Chen, B. Zhou, L. Zhang, W. Zhang, S. Wang and J. Zang, "Geometrical Evaluation on the Viscous Effect of Point-Absorber Wave-Energy Converters", *China Ocean Engineering*, vol. 32, no. 4, pp. 443-452, 2018.